Electric Field Manipulated Magnetic Spin Coupling Properties in Lithium-Trapped Nitrogen-Vacancy Nanodiamond

Zhuxiao Li, Zhiru Zhang, Yuxiang Bu, Xinyu Song*

School of Chemistry and Chemical Engineering, Shandong University, Jinan 250100, People's Republic of China. E-mail: songxy@sdu.edu.cn

Supplementary Material

Section S1. Details of Evaluating Components of the Effects of External Electric Field

The superscript of $\boldsymbol{R}$ denotes whether the geometric structure is optimized under an external electric field (EF), and the superscript of ψ denotes whether the electron distribution is calculated under an EF. Therefore, the structure of clusters is optimized and calculated without an EF in the C···Li direction, its electron distribution and structure are denoted as $\psi^0(\boldsymbol{R}^0)$. The structure of clusters is optimized and calculated with an EF in the C···Li direction, denoted as NVLi-C, and its electron distribution and structure are denoted as $\psi^F(\boldsymbol{R}^F)$. The structure of clusters is optimized and calculated with an EF in the N···Li direction, denoted as NVLi-N. The structure of clusters is optimized with an EF in the C···Li direction, but the electron distribution is calculated at a single point without an EF, denoted as NVLi-C-SP, and its electron distribution and structure are denoted as $\psi^0(\boldsymbol{R}^F)$. They have the following relationship:

$$\psi^0(\boldsymbol{R}^0) \xrightarrow{-\text{structure deformation}} \psi^0(\boldsymbol{R}^F) \xrightarrow{-\text{electron relaxation}} \psi^F(\boldsymbol{R}^F)$$

The total effect of EF on clusters can be obtained by analyzing $\psi^0(\boldsymbol{R}^0)$ and $\psi^F(\boldsymbol{R}^F)$. The indirect effect of EF on electrons by acting on geometric structure can be obtained by analyzing $\psi^0(\boldsymbol{R}^0)$ and $\psi^0(\boldsymbol{R}^F)$. The direct effect of EF on electrons under the same structure can be obtained by analyzing the difference between $\psi^0(\boldsymbol{R}^F)$ and $\psi^F(\boldsymbol{R}^F)$.

In addition, the structure of clusters is optimized without an EF in the C···Li direction, but the electron distribution is calculated at a single point with an EF, its electron distribution and structure are denoted as $\psi^F(\boldsymbol{R}^0)$, which can be used to analyze the atomic force.

$$\psi^0(\boldsymbol{R}^0) \xrightarrow{-\text{relaxation}} \psi^F(\boldsymbol{R}^0)$$

Section S2. Structural Deformation and Electron Relaxation

The change of dipole moment in EF is a simple and direct index to measure the degree of polarization of the cluster. From the dipole moment of the NVLi-C-SP ($\psi^0(\boldsymbol{R}^F)$, Section S1) and the NVLi-C ($\psi^F(\boldsymbol{R}^F)$, Section S1), it can be clearly seen that the induced dipole moment formed by the polarization electrons changes significantly (Figure S1a).

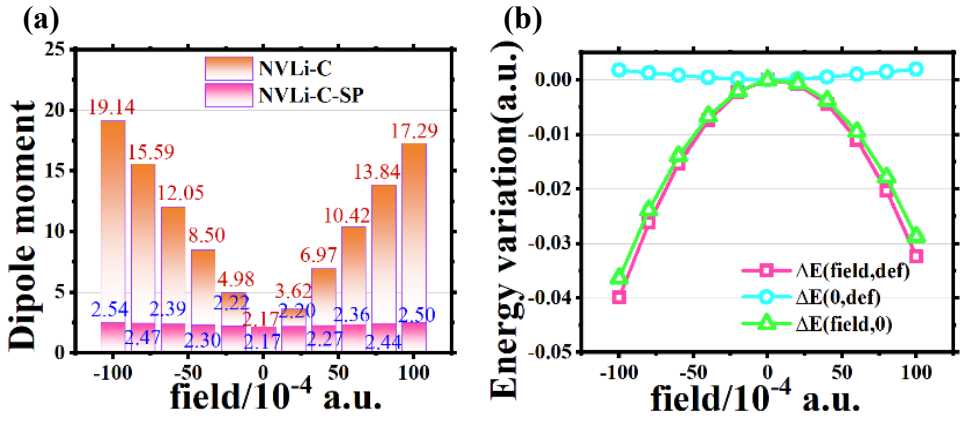

Figure S1 (**a**) The change of the overall dipole moment of NVLi-C and NVLi-C-SP; (**b**) The ground state energy change after deformation or polarization is caused by different EF (along the C1···Li direction), including $\Delta E[\psi^F(\boldsymbol{R}^F)]$, $\Delta E[\psi^0(\boldsymbol{R}^F)]$, $\Delta E[\psi^F(\boldsymbol{R}^0)]$.

It can be seen from the energy change diagram (Figure S1b) that the energy increase caused by the structural deformation is much lower than the energy decrease caused by the electron relaxation in EF. However, the change of J value is also significant when only the structural deformation is considered (NVLi-C-SP, Table S1, Table S2), which shows that both structural deformation and electron relaxation are the important factors affecting J value, neither can be ignored.

Section S3. Origin of Structural Deformation

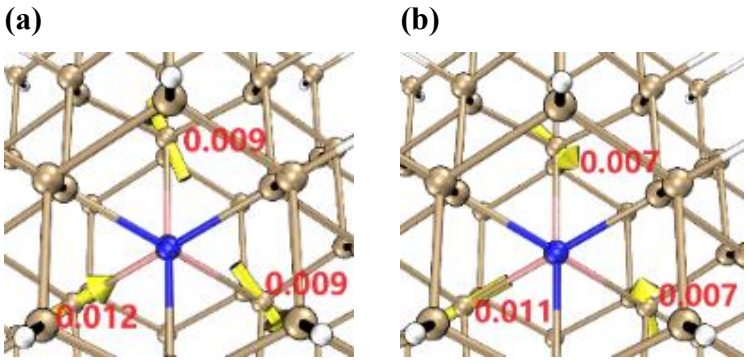

Figure S2 (**a**) When EF is -0.01 a.u. (along the C1···Li direction), the force of C radical; (**b**) When EF is 0.01 a.u. (along the C1···Li direction), the force of C radical;

The direct cause of structural deformation is resulted from the force on the atoms. The force direction of the atoms can be observed by applying an electric field to the fixed structure, and then the factors such as the change of the atomic distances can be analyzed. The atomic force diagram shows that when EF < 0, the force direction of C1 points to the Li atom, while the force of C2 and C3 has the main component opposite to each other (Figure S2a**)**. On the contrary, when EF > 0, the force of C1 deviates from the Li atom, while the force of C2 and C3 has the main component face to each other (Figure S2b**)**.

The change of the force is due to the change of the components of the Coulomb force on the atom, which comes from the significantly change of electron cloud distribution under the EF (Figure 6a-b, Figure S1). When no EF is applied, the electron cloud is uniformly delocalized on three C radicals. When EF < 0, the electron cloud is mainly distributed between C1 and Li (Figure 6a). It can be considered that the repulsion of the C1 nucleus by Li^+ cation is shielded by the delocalized electron cloud, so the C1 is subjected to the force pointing to Li. The electron cloud density between C2 and C3 is reduced, which weakens the shielding effect and enhances the repulsion between C2 and C3. Therefore, the distance between C2···C3 when EF < 0 is larger than that without the EF, while the distance between C1···C2 and C1···C3 is smaller than that without the EF. When EF > 0, the situation is opposite (Figure 6b). In addition, the Li^+ cation is directly affected by EF because of its positive net charge.

Section S4. Qualitative Analysis of SOMO Overlap and Approximate Orbital Interaction

Some studies have pointed out that when the SOMOs overlap, the system exhibits ferromagnetism (FM), and when SOMOs doesn't overlap, the system exhibits antiferromagnetism (AFM). However, it is noted that the qualitative analysis cannot well indicate the change of SOMOs overlapping under the change of EF. In addition, it is obvious that the Coulomb integral and exchange integral between orbits is positively correlated with the degree of overlap between orbits, and we know that the Coulomb integral and exchange integral between orbits can quantitatively describe the factors of orbital interaction in magnetic coupling. Therefore, the SOMOs overlapping is quantified and its relationship with the Coulomb integral and exchange integral between SOMOs is analyzed.

The overlap integral of square of the two orbitals (the electron density on the orbits) can accurately and quantitatively measure the degree of overlap between the orbits. The expression is as follows:

$$\int |\varphi_i(\boldsymbol{r})|^2 |\varphi_j(\boldsymbol{r})|^2 d\boldsymbol{r}$$

This formula shows that the product of the composition ratios of the two orbitals on the same atom can be approximately considered as the overlap on the atom, so the sum of the product of the composition ratios of the two orbitals of all the atoms can approximately measure the degree of overlap between the two orbitals. Considering that SOMOs are mainly distributed on three C radicals, only the sum of the product of the two SOMOs components on the C radicals is calculated. The above-mentioned related quantities are linearly fitted, and they all show a good linear positive correlation (Figure S9). Therefore, the sum of the product of the proportion of C radicals in the two SOMOs components can be used to approximately represent the Coulomb integral and the exchange integral.

Section S5. Other Calculational Results

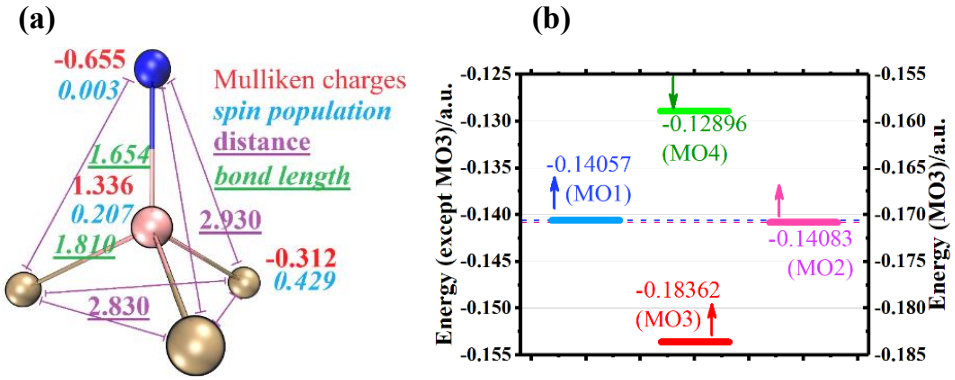

Figure S3 (**a**) Structure, Mulliken charges (red) and spin populations (blue) at N, Li and C, and interatomic distances of adjacent atoms of the NVLi center; (**b**) The orbital energy of four outer occupied orbitals of NVLi-C in the T ground state without EF.

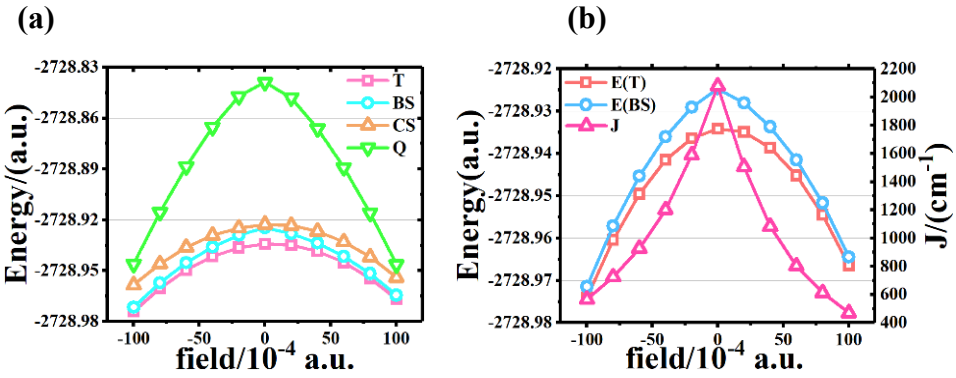

Figure S4 (**a**) The energies of the NVLi cluster in the T, BS, CS and Q state vary with EF (along the C1···Li direction); (**b**) The triplet (T), symmetry-breaking singlet (BS) energy and magnetic coupling constant (*J*) change with EF (along the C···Li direction).

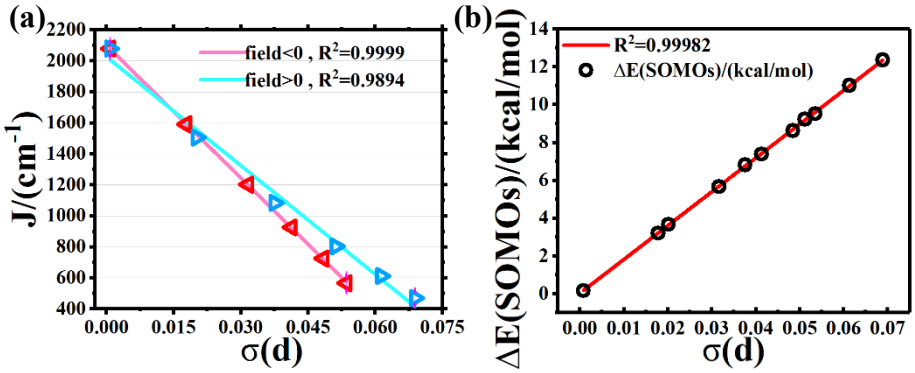

Figure S5 (**a**) Linear correlation of the magnetic coupling constant (*J*) with the standard deviation of the distances of C radicals (σ(d)), which is defined as: $\sigma(d) = \sqrt{\frac{\sum_{i\neq j}^{n}(d_{ij}-\bar{d})^2}{n}}$; (**b**) The linear correlation between ΔE_{SOMOs} and the standard deviation of the distances of C radicals (σ(d)) of NVLi-C-SP.

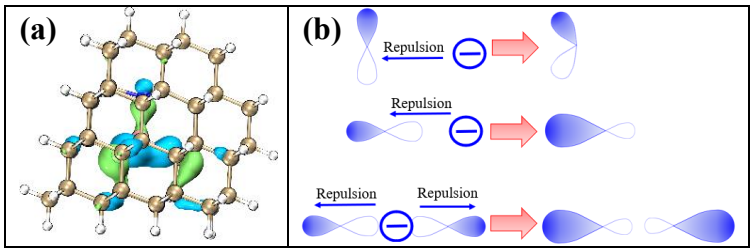

Figure S6 (**a**) MO3 orbital distribution isosurface side view; (**b**) The diagram of polarization deformation of the orbit due to the repulsion from EF or electric cloud.

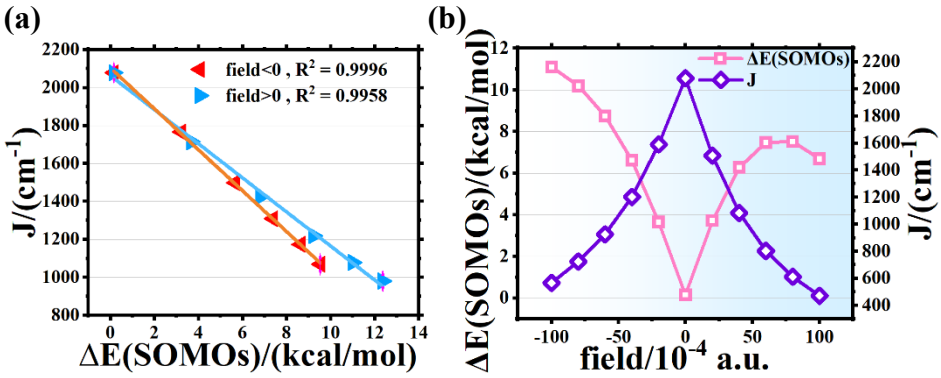

Figure S7 (**a**) ΔE_{SOMOs} and *J* value linear fitting of NVLi-C-SP; (**b**) The change of ΔE_{SOMOs} and *J* value with EF (along the C1···Li direction) of NVLi-C.

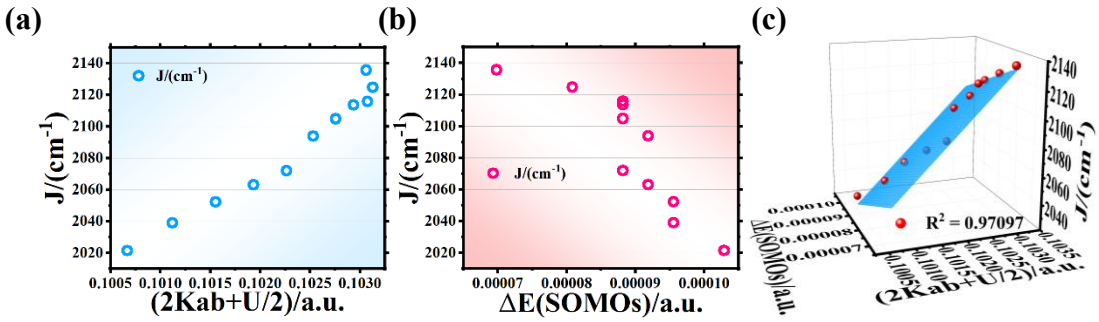

Figure S8 (**a**) The association between J and SOMOs interaction $(2K_{ab} + \frac{U}{2})$ of NVLi-N; (**b**) The correlation between J and ΔE_{SS} of NVLi-N; (**c**) The plane fitting of J with the two terms of eq 5 of NVLi-N, rotated along the Z-axis to make the fitted plane more pronounced.

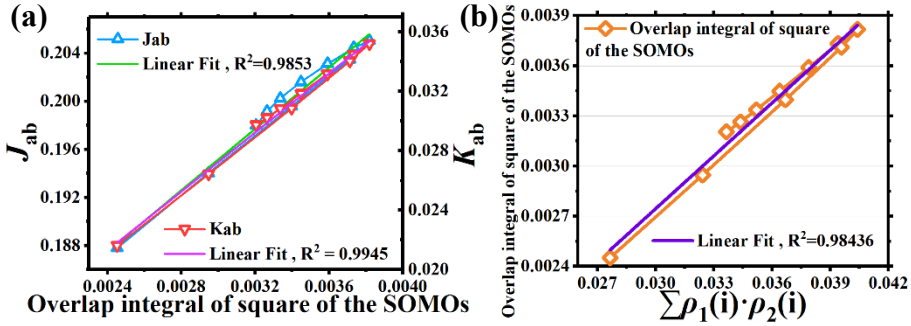

Figure S9 (**a**) The linear fit between the Coulomb integral (J_{ab}) and the overlap integral of square, the exchange integral (K_{ab}) and the overlap integral of square between SOMOs; (**b**) A linear fit between the overlap integral of square between SOMOs and the sum of the product of the contributions of the same atom of the two SOMO components.

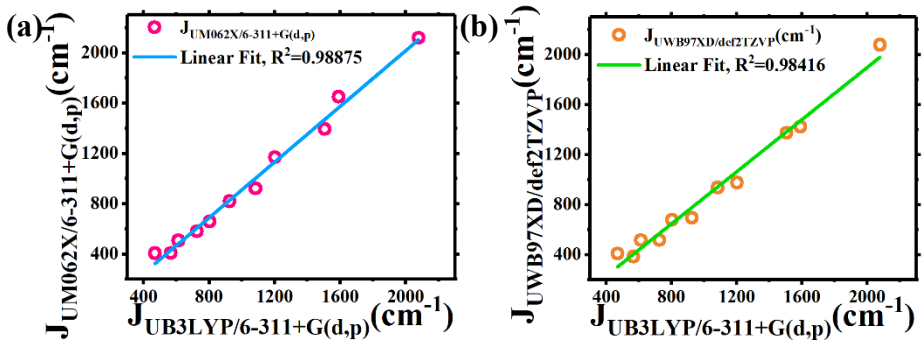

Figure S10 (**a**) The linear correlation between the magnetic coupling constant (J, at the (U)M062X/6-311+G (d, p) level) and J (at the (U)B3LYP/6-311+G (d, p) level) for NVLi-C; (**b**) The linear correlation between J (at the (U)ωB97XD/def2TZVP level) and J (at the (U)B3LYP/6-311+G (d, p) level) for NVLi-C.

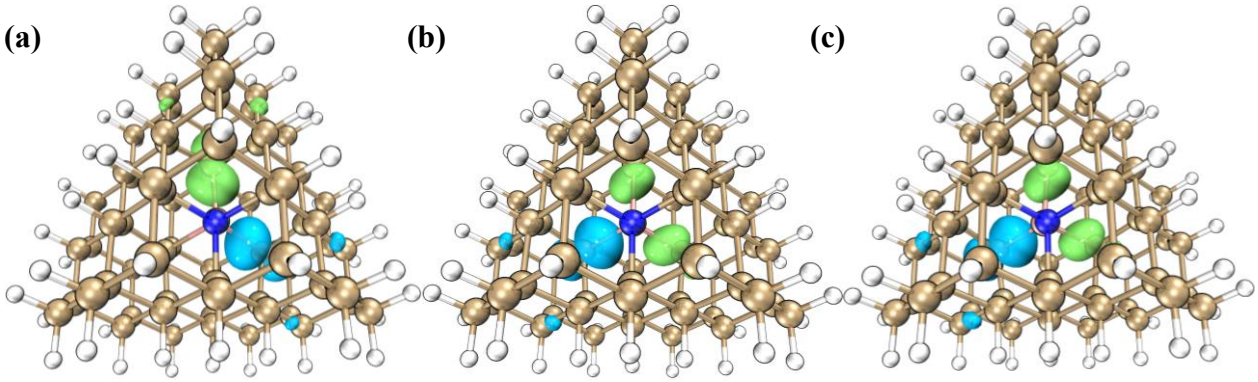

Figure S11 Isosurfaces of spin density distributions of BS state of NVLi-C at EF of -0.01a.u. (**a**), 0 a.u. (**b**) and 0.01a.u. (**c**), respectively.

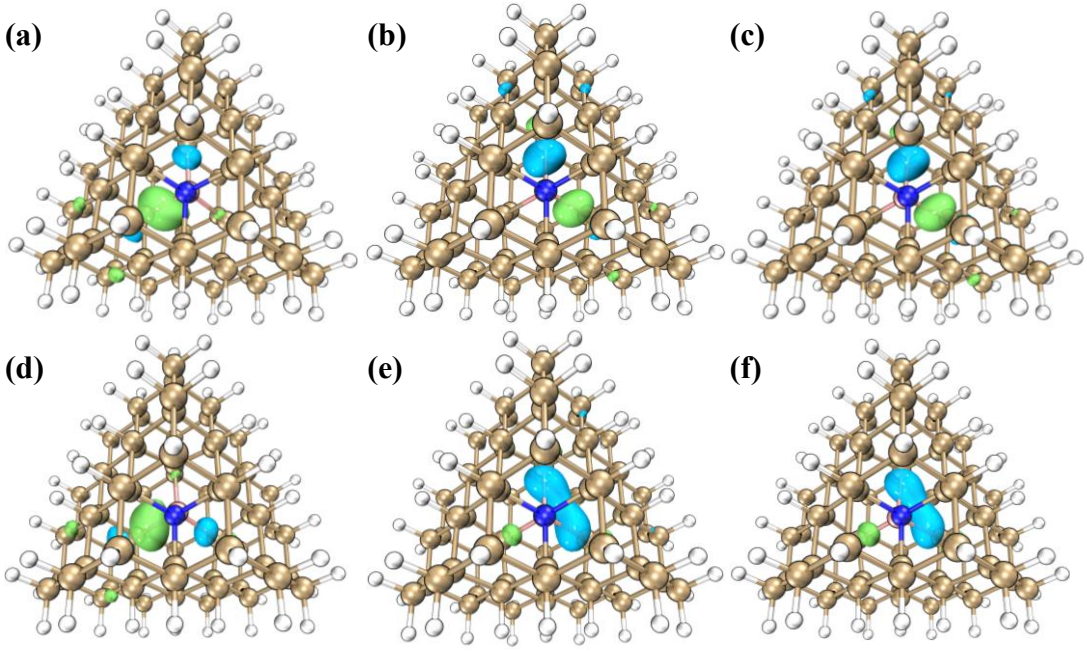

Figure S12 (**a-c**) The isosurface diagrams of SOMOα distributions of BS state of NVLi-C at EF of -0.01 a.u., 0 a.u. and 0.01 a.u., respectively; (**d-f**) The isosurface diagrams of SOMOβ distributions of BS state of NVLi-C at EF of -0.01a.u., 0 a.u. and 0.01a.u., respectively.

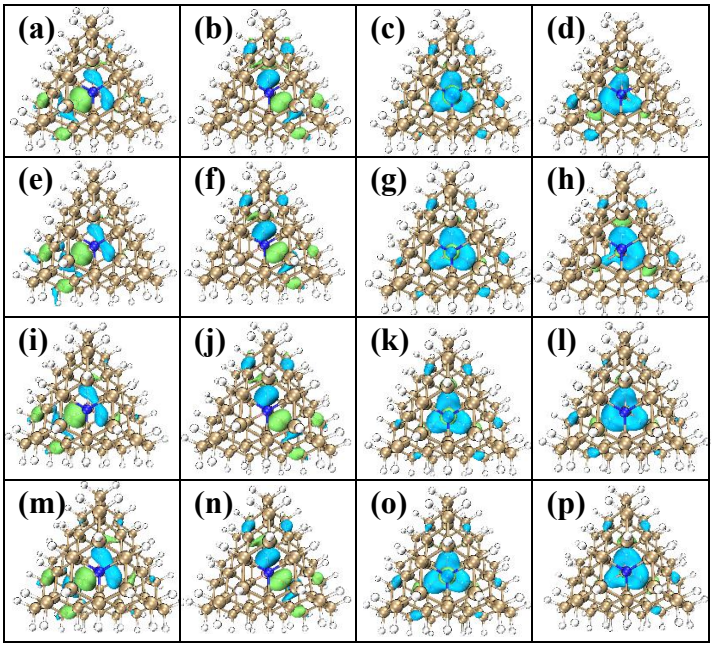

Figure S13 EF effect on FMO distributions. (**a-d**) The isosurface diagrams of FMO distributions of NVLi-C under EF = -0.01 a.u.; (**e-h**) Those of NVLi-C under EF = 0.01 a.u.; (**i-l**) Those of NVLi-C-SP without EF but at the geometry deformed by EF (-0.01 a.u.); (**m-p**) Those of NVLi-C-SP without EF but at the geometry deformed by EF (0.01 a.u.)

Table S1. The energy (E), the squared eigenvalue of spin angular momentum (<S^2>) and the magnetic coupling constant (J) of NVLi-C.

field/10^{-4}a.u.	E_T/a.u. ($< S^2 >_T$)	E_{BS}/a.u. ($< S^2 >_{BS}$)	J(cm^{-1})
-100	-2728.97405(2.010)	-2728.97146(1.007)	566.74
-80	-2728.96040(2.010)	-2728.95708(1.005)	725.03
-60	-2728.94955(2.010)	-2728.94530(1.003)	926.28
-40	-2728.94153(2.010)	-2728.93601(1.002)	1201.88
-20	-2728.93638(2.010)	-2728.92907(1.001)	1590.05
0	-2728.93416(2.010)	-2728.92468(1.009)	2078.54
20	-2728.93492(2.010)	-2728.92805(1.009)	1506.28
40	-2728.93861(2.010)	-2728.93367(1.009)	1083.12
60	-2728.94516(2.010)	-2728.94150(1.010)	803.28
80	-2728.95447(2.010)	-2728.95168(1.010)	612.33
100	-2728.96653(2.010)	-2728.96442(1.025)	470.14

Table S2. The energy (E), the squared eigenvalue of spin angular momentum (<S^2>) and the magnetic coupling constant (J) of NVLi-C-SP.

field/10^{-4}a.u.	E_T/a.u. ($< S^2 >_T$)	E_{BS}/a.u. ($< S^2 >_{BS}$)	J(cm^{-1})
-100	-2728.93238(2.010)	-2728.92738(0.983)	1068.52
-80	-2728.93285(2.010)	-2728.92737(0.985)	1173.39
-60	-2728.93329(2.010)	-2728.92719(0.987)	1308.70
-40	-2728.93370(2.010)	-2728.92674(0.991)	1499.06
-20	-2728.93402(2.010)	-2728.92586(0.996)	1766.19
0	-2728.93416(2.010)	-2728.92468(1.009)	2078.54
20	-2728.93401(2.010)	-2728.92619(1.009)	1714.58
40	-2728.93363(2.010)	-2728.92713(1.009)	1425.16
60	-2728.93315(2.010)	-2728.92759(1.009)	1219.06
80	-2728.93266(2.010)	-2728.92774(1.009)	1078.74
100	-2728.93218(2.010)	-2728.92771(1.009)	980.07

Table S3. The spin populations at N, C radicals and Li under different EFs of NVLi-C, based on Becke 's population analysis.

field/10^{-4}a.u.	N	C1	C2	C3	Li
-100	0.00272	0.22400	0.52552	0.52498	0.20575
-80	0.00281	0.25614	0.51162	0.51086	0.20561
-60	0.00289	0.29153	0.49557	0.49450	0.20590
-40	0.00293	0.33193	0.47670	0.47527	0.20622
-20	0.00294	0.37832	0.45432	0.45255	0.20662
0	0.00293	0.42871	0.42899	0.42710	0.20712
20	0.00293	0.47639	0.40393	0.40224	0.20759
40	0.00293	0.51278	0.38384	0.38260	0.20793
60	0.00289	0.53700	0.36971	0.36874	0.20828
80	0.00284	0.55217	0.36011	0.35926	0.20859
100	0.00283	0.56169	0.35409	0.35327	0.20864

Table S4. The internuclear distance of C···Li and N···Li under different intensities of NVLi-N.

field/10^{-4}a.u.	$d_{(N\cdots Li)}$/Å	$d_{(C1\cdots Li)}$/Å	$d_{(C2\cdots Li)}$/Å	$d_{(C3\cdots Li)}$/Å
-100	1.66247	1.80804	1.80831	1.80775
-80	1.65818	1.80914	1.80943	1.80886
-60	1.65712	1.80936	1.80965	1.80908
-40	1.65611	1.80961	1.80990	1.80932
-20	1.65515	1.80988	1.81017	1.80959
0	1.65428	1.81014	1.81045	1.80987
20	1.65339	1.81049	1.81079	1.81019
40	1.65260	1.81082	1.81113	1.81053
60	1.65187	1.81119	1.81149	1.81089
80	1.64960	1.81216	1.81246	1.81186
100	1.64725	1.81327	1.81356	1.81296

Table S5. The internuclear distance of N-Cand C-C under different intensities of NVLi-N.

field/10^{-4}a.u.	$d_{(N\cdots C1)}$/Å	$d_{(N\cdots C2)}$/Å	$d_{(N\cdots C3)}$/Å	$d_{(C1\cdots C2)}$/Å	$d_{(C1\cdots C3)}$/Å	$d_{(C2\cdots C3)}$/Å
-100	2.93328	2.93281	2.93348	2.83044	2.83119	2.83080
-80	2.93233	2.9319	2.93254	2.82977	2.83046	2.83013
-60	2.93182	2.93139	2.93203	2.82985	2.83053	2.83021
-40	2.93138	2.93096	2.93159	2.82996	2.83063	2.83032
-20	2.93102	2.93059	2.93122	2.83009	2.83076	2.83045
0	2.93072	2.93030	2.93093	2.83025	2.83092	2.83062
20	2.93050	2.93008	2.93070	2.83045	2.83110	2.83080
40	2.93035	2.92993	2.93055	2.83066	2.83131	2.83101
60	2.93027	2.92986	2.93047	2.83090	2.83155	2.83125
80	2.93008	2.92967	2.93027	2.83119	2.83180	2.83150
100	2.93083	2.93044	2.93102	2.83037	2.83090	2.83063

Table S6. The contribution of atoms to the composition of MO1 of NVLi-N.

field/10^{-4}a.u.	C1	C2	C3	N	Li
-100	16.678	26.314	2.087	0.581	3.883
-80	17.390	26.077	1.864	0.581	3.872
-60	17.520	26.162	1.852	0.580	3.866
-40	17.654	26.228	1.835	0.580	3.859
-20	17.806	26.267	1.809	0.580	3.850
0	17.995	26.265	1.768	0.580	3.840
20	18.040	26.344	1.774	0.581	3.828
40	18.115	26.387	1.765	0.582	3.815
60	18.207	26.403	1.749	0.584	3.801
80	18.218	26.463	1.756	0.586	3.781
100	18.267	26.488	1.751	0.588	3.758

Table S7. The contribution of atoms to the composition of MO2 of NVLi-N.

field/10^{-4}a.u.	C1	C2	C3	N	Li
-100	13.364	3.749	27.938	0.580	3.881
-80	12.821	4.152	28.332	0.580	3.870
-60	12.826	4.202	28.480	0.580	3.864
-40	12.816	4.257	28.620	0.579	3.857
-20	12.774	4.328	28.757	0.579	3.848
0	12.683	4.427	28.896	0.580	3.838
20	12.724	4.434	28.978	0.580	3.827
40	12.722	4.464	29.061	0.581	3.814
60	12.691	4.508	29.138	0.583	3.800
80	12.733	4.500	29.185	0.586	3.781
100	12.730	4.521	29.239	0.588	3.757

Table S8. The contribution of atoms to the composition of MO3 of NVLi-N.

field/10^{-4}a.u.	C1	C2	C3	N	Li
-100	13.430	13.421	13.433	1.648	4.316
-80	13.353	13.345	13.355	1.863	4.302
-60	13.213	13.205	13.215	2.212	4.274
-40	13.004	12.996	13.007	2.695	4.232
-20	12.695	12.686	12.697	3.383	4.170
0	12.232	12.222	12.235	4.393	4.080
20	11.538	11.527	11.541	5.902	3.948
40	10.506	10.493	10.508	8.161	3.762
60	9.045	9.031	9.048	11.391	3.513
80	7.263	7.248	7.266	15.354	3.229
100	5.346	5.331	5.349	19.640	2.946

Table S9. The contribution of atoms to the composition of MO4 of NVLi-N.

field/10^{-4}a.u.	C1	C2	C3	N	Li
-100	15.285	15.343	15.246	0.670	5.659
-80	15.309	15.358	15.269	0.676	5.666
-60	15.319	15.366	15.280	0.696	5.671
-40	15.324	15.368	15.286	0.720	5.674
-20	15.323	15.365	15.287	0.750	5.674
0	15.317	15.354	15.279	0.786	5.673
20	15.300	15.337	15.265	0.830	5.669
40	15.274	15.309	15.241	0.886	5.663
60	15.237	15.269	15.204	0.957	5.652
80	15.187	15.216	15.158	1.038	5.638
100	15.120	15.145	15.095	1.138	5.618

Table S10. The atomic spin population of NVLi-N.

field/10^{-4}a.u.	N	C1	C2	C3	Li
-100	-0.006	0.542	0.541	0.543	0.161
-80	-0.006	0.545	0.544	0.545	0.157
-60	-0.005	0.546	0.545	0.547	0.154
-40	-0.005	0.548	0.547	0.549	0.151
-20	-0.005	0.550	0.549	0.550	0.147
0	-0.005	0.551	0.551	0.552	0.144
20	-0.005	0.553	0.552	0.553	0.141
40	-0.005	0.555	0.554	0.555	0.138
60	-0.005	0.556	0.555	0.556	0.135
80	-0.004	0.558	0.557	0.558	0.131
100	-0.004	0.559	0.559	0.559	0.127

Table S11. The ΔE_{SOMOs} of clusters under different conditions.

field/10^{-4}a.u.	ΔE_{SOMOs} of NVLi-N /(kcal/mol)	ΔE_{SOMOs} of NVLi-C-SP /(kcal/mol)	ΔE_{SOMOs} of NVLi-C /(kcal/mol)
-100	0.065	9.53	11.11
-80	0.060	8.63	10.19
-60	0.060	7.39	8.75
-40	0.058	5.67	6.62
-20	0.055	3.21	3.65
0	0.058	0.16	0.16
20	0.055	3.67	3.72
40	0.055	6.82	6.27
60	0.055	9.23	7.47
80	0.051	11.02	7.52
100	0.044	12.37	6.69

Table S12. The energy (E), the squared eigenvalue of spin angular momentum (<S^2>) and the magnetic coupling constant (J) of NVLi-N.

field/10^{-4}a.u.	E_T/a.u. ($< S^2 >_T$)	E_{BS}/a.u. ($< S^2 >_{BS}$)	J(cm^{-1})
-100	-2728.94876(2.010)	-2728.93954(1.009)	2021.53
-80	-2728.93947(2.010)	-2728.93017(1.009)	2039.07
-60	-2728.93265(2.010)	-2728.92329(1.009)	2052.23
-40	-2728.92827(2.010)	-2728.91886(1.009)	2063.19
-20	-2728.92631(2.010)	-2728.91686(1.009)	2071.96
0	-2728.92679(2.010)	-2728.91724(1.009)	2093.89
20	-2728.92970(2.010)	-2728.92010(1.009)	2104.85
40	-2728.93505(2.010)	-2728.92541(1.009)	2113.62
60	-2728.94283(2.010)	-2728.93318(1.009)	2115.81
80	-2728.95308(2.011)	-2728.94338(1.009)	2124.65
100	-2728.96578(2.011)	-2728.95603(1.009)	2135.61

Table S13. The ΔE_{SOMOs} and the standard deviation of the distances of C radicals ($\sigma(d) = \sqrt{\frac{\sum_{i\neq j}^{n}(d_{ij}-\bar{d})^2}{n}}$) of NVLi-C-SP.

field/10^{-4}a.u.	σ(d) /Å	ΔE_{SOMOs}/(kcal/mol)
-100	0.05352	9.53
-80	0.04845	8.63
-60	0.04131	7.39
-40	0.03162	5.67
-20	0.01778	3.21
0	0.00080	0.16
20	0.02014	3.67
40	0.03755	6.82
60	0.05115	9.23
80	0.06126	11.02
100	0.06887	12.37

Table S14. The SOMOs interaction ($2K_{ab} + \frac{U}{2}$).

field/10^{-4}a.u.	NVLi-N /a.u.	NVLi-C-SP /a.u.	NVLi-C /a.u.
-100	0.10067	0.10643	0.10722
-80	0.10112	0.10648	0.10767
-60	0.10155	0.10672	0.10805
-40	0.10193	0.10714	0.10847
-20	0.10226	0.10777	0.1089
0	0.10253	0.10223	0.10223
20	0.10276	0.10423	0.10359
40	0.10294	0.10623	0.10191
60	0.10308	0.10801	0.0969
80	0.10313	0.10956	0.08956
100	0.10306	0.11096	0.07857

Table S15. The energy (E), the squared eigenvalue of spin angular momentum (<S^2>) and the magnetic coupling constant (J) of NVLi-C at the (U)M062X/6-311+G (d, p) level.

field/10^{-4}a.u.	E_T/a.u. ($< S^2 >_T$)	E_{BS}/a.u. ($< S^2 >_{BS}$)	J(cm^{-1})
-100	-2727.59413(2.010)	-2727.59227(1.010)	408.22
-80	-2727.58025(2.010)	-2727.57760(1.010)	581.61
-60	-2727.56918(2.011)	-2727.56544(1.009)	819.20
-40	-2727.56099(2.011)	-2727.55565(1.009)	1169.66
-20	-2727.55575(2.012)	-2727.54821(1.010)	1651.54
0	-2727.55350(2.012)	-2727.54384(1.011)	2118.01
20	-2727.55433(2.011)	-2727.54798(1.011)	1393.66
40	-2727.55826(2.011)	-2727.55406(1.011)	921.79
60	-2727.56511(2.011)	-2727.56211(1.011)	658.42
80	-2727.57462(2.011)	-2727.57231(1.012)	507.49
100	-2727.58669(2.011)	-2727.58484(1.013)	406.84

Table S16. The energy (E), the squared eigenvalue of spin angular momentum (<S^2>) and the magnetic coupling constant (J) of NVLi-C at the (U)ωB97XD/def2TZVP level.

field/10^{-4}a.u.	E_T/a.u. ($< S^2 >_T$)	E_{BS}/a.u. ($< S^2 >_{BS}$)	J(cm^{-1})
-100	-2728.15516(2.011)	-2728.15341(1.011)	384.08
-80	-2728.14126(2.011)	-2728.13891(1.011)	515.77
-60	-2728.13000(2.012)	-2728.12683(1.011)	695.04
-40	-2728.12145(2.012)	-2728.11700(1.011)	975.69
-20	-2728.11578(2.013)	-2728.10928(1.011)	1423.74
0	-2728.11332(2.013)	-2728.10385(1.013)	2078.42
20	-2728.11430(2.013)	-2728.10804(1.013)	1373.91
40	-2728.11840(2.013)	-2728.11413(1.013)	937.16
60	-2728.12522(2.012)	-2728.12213(1.013)	678.86
80	-2728.13459(2.012)	-2728.13224(1.013)	516.28
100	-2728.14647(2.012)	-2728.14461(1.013)	408.63

Table S17. The spin populations at N, C radicals and Li under different EFs of BS state of NVLi-C, based on Becke 's population analysis.

field/10^{-4} a.u.	N	C1	C2	C3	Li
-100	-0.00001	-0.00105	0.54176	-0.54095	0.00014
0	-0.00019	-0.55328	0.29250	0.26703	-0.00116
100	0.00101	-0.57954	0.32322	0.32206	-0.00917